Enhanced Hole Extraction in Perovskite Solar Cells Through Carbon Nanotubes

ARTICLE *in* JOURNAL OF PHYSICAL CHEMISTRY LETTERS · DECEMBER 2014

Impact Factor: 7.46 · DOI: 10.1021/jz5021795

THE JOURNAL OF PHYSICAL CHEMISTRY Letters

Letter

pubs.acs.org/JPCL

Enhanced Hole Extraction in Perovskite Solar Cells Through Carbon Nanotubes

Severin N. Habisreutinger, Tomas Leijtens, Giles E. Eperon, Samuel D. Stranks, Robin J. Nicholas, and Henry J. Snaith*

Department of Physics, Clarendon Laboratory, University of Oxford, Parks Road, Oxford OX1 3PU, United Kingdom

Supporting Information

ABSTRACT: Here, we report the use of polymer-wrapped carbon nanotubes as a means to enhance charge extraction through undoped spiro-OMeTAD. With this approach a good solar cell performance is achieved without the implementation of conventional doping methods. We demonstrate that a stratified two-layer architecture of sequentially deposited layers of carbon nanotubes and spiro-OMeTAD, outperforms a conventional blend of the hole-conductor and the carbon nanotubes. We also provide insights into the mechanism of the rapid hole extraction observed in the two-layer approach.

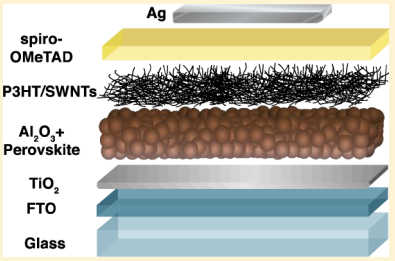

SECTION: Energy Conversion and Storage; Energy and Charge Transport

Over the past four years, the performance of perovskite solar cells has skyrocketed.[1,2] The perovskite material $CH_3NH_3PbI_3$ made from mixed halide precursors has the remarkable ability to function both as a wide-range absorber and as an ambipolar charge transporter.[3−5] It can therefore be coated onto an electronically inert alumina scaffold resulting in 'meso-superstructured solar cells' (MSSCs) in which charge generation and transport both happen within the perovskite material.[4] After photogeneration, both electrons and holes reside in the bulk of the perovskite. For efficient charge extraction with minimal recombination losses, the perovskite layer needs to be contacted with charge-selective n-type and p-type materials, which exhibit low resistive losses. Currently, the best performing devices employ a p-type organic hole-conductor, 2,2′,7,-7′-tetrakis(*N*,*N*-di-*p*-methoxyphenylamine)-9,9′-spirobifluorene (spiro-OMeTAD) as the hole transport layer (HTL). The low intrinsic charge carrier mobility of amorphous organic hole-conductors can be overcome to a certain extent by increasing the carrier density via oxidative doping.[6−8] However, we have demonstrated previously that the stability of a perovskite solar cell depends crucially on the ability of the hole-transporter to withstand the ingress of moisture at elevated temperatures.[9] In particular, in the presence of hygroscopic dopants such as lithium bis-(trifluoromethane)sulfonimide (Li-TFSI), moisture-induced degradation is significantly accelerated. By using a protective polymer matrix to prevent moisture ingress in conjunction with single-walled carbon nanotubes (SWNTs) for charge extraction, we demonstrated a strategy to significantly improve the overall stability of perovskite solar cells.[9]

In the following study, we elucidate the rationale and basic mechanism for employing a two-layered structure of polymer-wrapped carbon nanotubes embedded within an organic matrix, and show that the nanotubes can fully replace the doping previously required for efficient devices. As a model system for the organic matrix, we use undoped spiro-OMeTAD, which can conduct holes but at much slower rates as compared to carbon nanotubes. Using the device performance of perovskite solar cells as well as photoinduced absorption spectroscopy and small perturbation photocurrent decays; we propose a mechanism for the observed enhancement in charge extraction in a two-layer approach. This architecture has the potential to serve as a model structure for a range of applications in which carbon nanotubes conduct charges.

We employ poly(3-hexylthiophene) (P3HT) wrapping to make the SWNTs dispersible in common solvents.[10] Such supramolecular nanohybrids (P3HT/SWNT) composed of SWNTs and a polymer-coating have been shown previously to enhance the performance of certain organic solar cells as additives.[11,12] Because the energy levels of the wrapping sheath of P3HT make the electron transfer from the perovskite to the SWNTs energetically unfavorable, the polymer coating should lead to selective hole-transfer to the nanotubes (Supporting Information).[11]

The solar cell structure employed in this study is shown schematically in Figure 1, where sequential layers of compact n-type TiO_2, mesoporous Al_2O_3, perovskite absorber, and SWNT-hole conductor composite are coated on to fluorine doped tin oxide (FTO) glass.

Figure 2 shows the current−voltage characteristics for representative devices in different configurations: without a hole-transport layer, with undoped spiro-OMeTAD, and with composites of neat spiro-OMeTAD and P3HT/SWNTs.

Received: October 14, 2014
Accepted: November 6, 2014
Published: November 6, 2014

   dx.doi.org/10.1021/jz5021795 | *J. Phys. Chem. Lett.* 2014, 5, 4207−4212

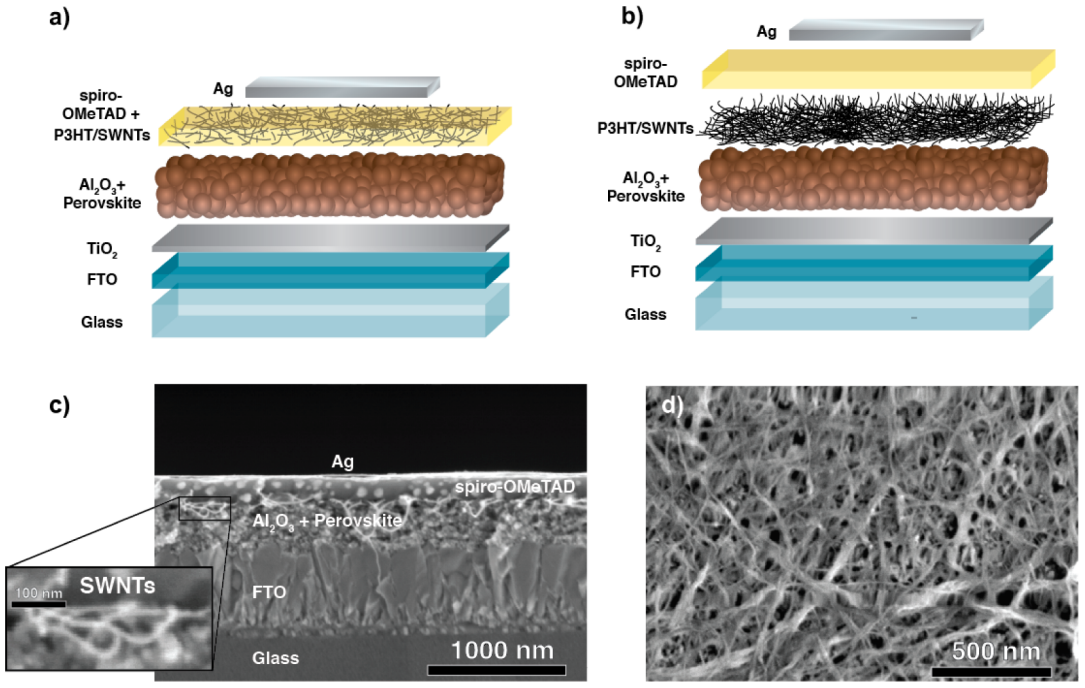

Figure 1. (a) Schematic of a device with a blend structure composed of undoped spiro-OMeTAD and P3HT/SWNTs. (b) Schematic architecture of a device with a P3HT/SWNT layer underneath the hole transport material (spiro-OMeTAD) matrix. (c) A cross-sectional scanning electron microscope (SEM) image of a representative device. Individual SWNTs can be seen to protrude from the interface between the alumina and spiro-OMeTAD layers. (d) Top view of a bare SWNT layer showing the thick mesh-like structure of the SWNT layer.

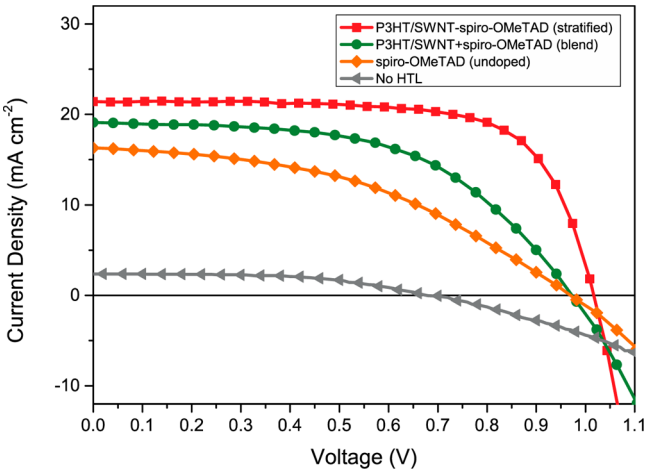

Figure 2. Comparison of current−voltage characteristics of two strategies of P3HT/SWNT incorporation into spiro-OMeTAD and two control structures. The presence of spiro-OMeTAD as the hole transport layer (orange diamonds) leads to a significant improvement in efficiency compared to the device without HTL (gray triangles). Dispersing P3HT/SWNTs in the spiro-OMeTAD layer further improve the JV-characteristics (green circles). However, the greatest improvement is achieved by sequential deposition of P3HT/SWNTs and spiro-OMeTAD (red squares), which results in a stratified HTL structure.

The device without a p-type collection layer, i.e., direct contact between the hole-collecting electrode and the perovskite layer, exhibits very poor current−voltage characteristics, with especially low short-circuit photocurrent. This suggests that direct metallic contact to the perovskite absorber in the MSSC structure, where both electrons and holes reside within the perovskite, is not advantageous for selective charge extraction. It has been shown that if the perovskite is coated onto an electron-accepting mesoporous layer of TiO_2, photogenerated holes are directly collected by a gold electrode.[13] This occurs as a result of rapid electron transfer to the mesoporous TiO_2 being more favorable than electron transfer to, or charge recombination at the gold electrode. However, the efficiency is significantly lower in this case.[14] Contrastingly, in the MSSC architecture electrons are not extracted as quickly, so electron transfer from the perovskite to the metal electrode is likely to occur, constituting a recombination pathway. The presence of a charge-selective hole contact can therefore reduce the recombination at the electrode by accepting holes but blocking electrons. Accordingly, we observe a significant improvement in efficiency even when undoped spiro-OMeTAD is used as the hole-collection layer. This reduced recombination is particularly evident in the enhanced open-circuit voltage and increased short-circuit photocurrent. Despite the low conductivity in the spiro-OMeTAD film, this configuration can still deliver a device with up to 16.3 mA/cm^2 photocurrent, but only 6.8% efficiency due to a poor fill factor (Figure 2, Table 1). Evidently, charge extraction is limited by the low mobility of the photogenerated charges inside the spiro-OMeTAD layer.

SWNTs are known for outstanding charge-carrier transport characteristics both on their own,[15−17] and also as additives which act to improve charge transport within polymer matrices.[18,19] In accordance with this, we find that dispersing P3HT/SWNTs within the spiro-OMeTAD layer results in a significant increase in device efficiency, which we ascribe to improved charge transport throughout the spiro-OMeTAD layer. In terms of device performance, this translates into an increase in the extracted photocurrent, as well as an improved fill factor and open-circuit voltage. This enhancement of performance parameters results in an efficiency increase to 10.0% (Figure 2, Table 1). However, compared to the

dx.doi.org/10.1021/jz5021795 | J. Phys. Chem. Lett. 2014, 5, 4207−4212

Table 1. Performance Parameters of Devices with Different Hole Transport Layers[a]

HTL architecture	J_{sc} [mA/cm^2]	V_{oc} [V]	FF	PCE [%]	Rs [Ω/cm^2]
no HTL	2.4	0.68	0.53	0.8	45.0
spiro-OMeTAD	16.3	0.97	0.43	6.8	16.9
P3HT/SWNT-spiro-OMeTAD (blend)	19.1	0.97	0.54	10.0	8.8
P3HT/SWNT-spiro-OMeTAD (stratified)	21.4	1.02	0.71	15.4	1.8

[a]These include two approaches of incorporating P3HT/SWNTs into the spiro-OMeTAD layer and two control structures.

performance parameters of state-of-the art MSSC perovskite solar cells, the photocurrent and fill factor are still low.[3,20,21] We suspect that in this configuration, the nanotubes cannot effectively form a closely interconnected percolation network that can effectively extend throughout the spiro-OMeTAD layer. This results in the device being limited by series resistance which in turn leads to a poor fill factor. Additionally, as they are randomly dispersed through the spiro-OMeTAD layer, the nanotubes may also not have enough direct interfacial contact to the perovskite absorber to efficiently transport holes away from the interface.

On the basis of these considerations, we investigated a second approach in which the nanotubes and spiro-OMeTAD are deposited sequentially. The initial deposition of the P3HT/SWNTs ensures that the nanotubes form a densely interconnected network with a direct contact to the perovskite layer, allowing efficient direct transfer of photogenerated holes from the absorber to the nanotubes. Subsequent coating and infilling with spiro-OMeTAD prevents the evaporated top electrode from directly contacting the perovskite, and forms the hole-conductor contact to the electrode. The nanotube network thus constitutes a highly conductive percolation network within the amorphous hole conductor matrix.

In Figure 1c we show a scanning electron microscopy (SEM) image of a representative device cross-section. P3HT/SWNT bundles are apparent protruding from the interface between the Al_2O_3-perovskite and spiro-OMeTAD layer. We assume that spiro-OMeTAD readily infiltrates the P3HT/SWNT layer, filling the openings and gaps of the mesh-like nanotube layer, due to its excellent pore filling properties and good wettability upon coating this surface. There is clearly stratification, with much higher P3HT/SWNT density near the perovskite surface, which should allow efficient charge transfer away from the interface. In fact, this is evident in the form of a much improved photocurrent in the current−voltage characteristics of a device with such a sequentially coated stratified P3HT/SWNT-spiro-OMeTAD composite layer, shown in Figure 2. The other significantly improved performance parameter is the fill factor, which can be attributed to fewer series resistance losses. This device yields a scanned power-conversion efficiency of 15.4% (Table 1).

It is clear that the stratified structure with the formation of a dense, interconnected network of P3HT/SWNT hybrids allows photogenerated holes from the perovskite to rapidly move through the horizontal plane to the most efficient vertical pathway to the top electrode. The fact that the devices work so well indicates that direct contact of the P3HT/SWNTs to the perovskite surface does not introduce an undesired electron recombination pathway, but instead facilitates selective hole transport.

As previously pointed out, perovskite solar cells often exhibit hysteretic current−voltage characteristics.[22,23] Changing the scanning conditions can therefore result in a change of the solar cell performance calculated from such a JV-curve. Determining the stabilized power output by holding a device at constant voltage around its maximum power point is an unambiguous performance metric for such devices.[22] We find that well-working devices usually have stabilized power output of around 0.8 of their scanned efficiency (Supporting Information).

In order to corroborate the proposed mechanism of charge extraction, we performed photoinduced absorption (PIA) spectroscopy. PIA is a quasi-continuous-wave (CW) technique, which enables probing the optical signature of photogenerated species. Because spiro-OMeTAD and P3HT/SWNTs exhibit different optical signatures when oxidized, it can be determined whether the photogenerated holes are residing on either component or both.

The PIA spectrum of a device with undoped spiro-OMeTAD HTL is shown in Figure 3a. The broad feature at ∼1300 nm is characteristic of the presence of holes in spiro-OMeTAD (i.e., its oxidized state).[4,24,25] For the stratified P3HT/SWNT-spiro-OMeTAD structure, we observe that the broad feature of oxidized spiro-OMeTAD becomes weaker and appears to be overlaid with a second, longer wavelength feature centered around 1450 nm. This suggests a smaller or shorter-lived hole population in the spiro-OMeTAD in the presence of P3HT/SWNTs. To isolate the specific features of P3HT/SWNTs in the PIA spectra, we carried out PIA measurements on devices with neat P3HT/SWNT films in place of spiro-OMeTAD. The resulting PIA spectrum is plotted in Figure 3b together with the absorption spectrum of a P3HT/SWNT film on glass. The absorption spectrum has the characteristic absorption peaks associated with the E_{11} transitions of s-type P3HT/SWNTs according to their chirality.[26] In the PIA spectrum, we observe a series of photobleaching (PB) features, which perfectly coincide with bleaching of the ground state absorption of the P3HT/SWNTs. The PIA absorption feature further into the infrared is presumably the absorption of the oxidized P3HT/SWNTs or electrons in the electron-accepting TiO_2 layer on the adjacent side of the perovskite film. The photobleaching features were not observed in PIA measurements on films of P3HT/SWNTs on glass without the active perovskite layer. We can thus exclude that the observed PB features are caused by charge transfer between the SWNTs and the encapsulating P3HT sheath.

To confirm that the photobleaching features observed in the PIA measurements do in fact correspond to the transfer of photogenerated holes to the SWNTs, we chemically p-doped functionalized SWNTs in solution using 2,3,5,6- tetrafluoro-7,7,8,8-tetracyanoquinodimethane (F_4TCNQ).[27] This chemical p-doping results in charge depletion of the SWNT valence bands. The change in absorbance between the undoped and the highly p-doped (oxidized) absorption spectrum (Figure 3a) shows a bleaching of the absorption of the ground state transitions (E_{11}), which closely resembles the photobleaching features detected in the PIA measurements (Figure 3c). We take this finding as evidence that the photobleaching features can be attributed to the injection of holes photogenerated in the perovskite absorber. These measurements show that the P3HT/SWNT nanohybrids act as an efficient hole-acceptor in their own right.

dx.doi.org/10.1021/jz5021795 | J. Phys. Chem. Lett. 2014, 5, 4207−4212

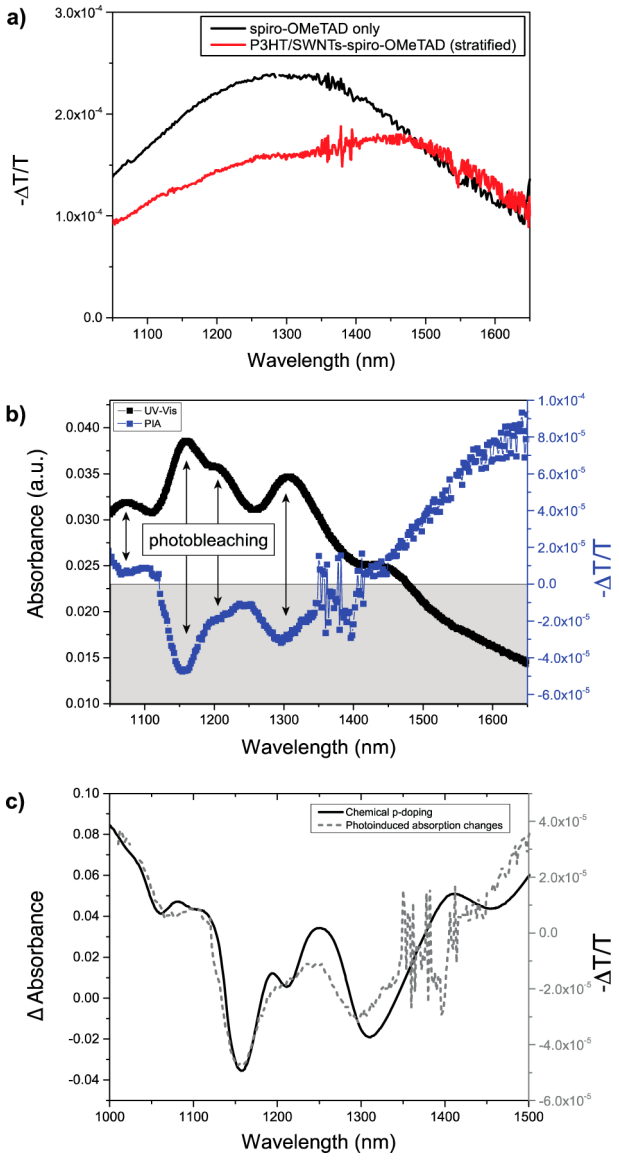

Figure 3. (a) The photoinduced-absorption (PIA) spectrum of both neat spiro-OMeTAD and the P3HT/SWNT-spiro-OMeTAD stratified HTL. The broad PIA feature at 1300 nm is characteristic of the presence of holes in spiro-OMeTAD. In the presence of the P3HT/SWNT interlayer, this feature appears to be much weaker and appears to be overlaid with a second, longer wavelength feature centered around 1450 nm. (b) The PIA spectrum of a device with a neat P3HT-wrapped P3HT/SWNT layer as HTL is plotted together with the absorption spectrum of a P3HT/SWNT film on glass. The photobleaching dips correspond well to the exciton absorption peaks of the s-type SWNTs from which hole injection from the perovskite into the P3HT/SWNT valence band can be inferred. (c) The absorption spectrum resulting from subtracting the absorption spectrum of undoped SWNTs and highly p-doped (oxidized) SWNTs in solution, overlaid with the photoinduced absorption spectrum of a P3HT/SWNT film on top of a perovskite absorber (excited at 515 nm).

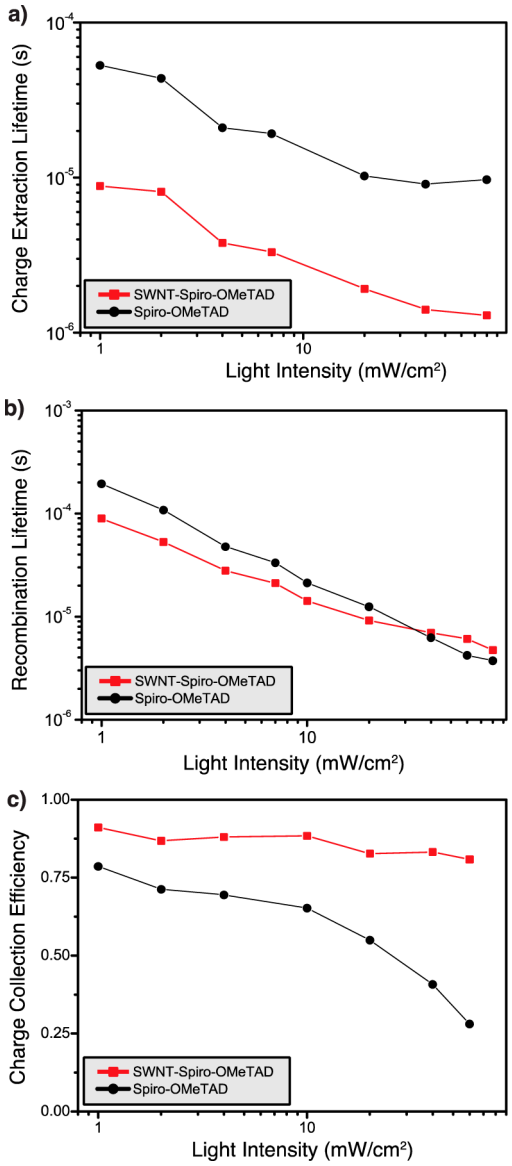

Figure 4. Results of the decay measurements of two devices with two different HTLs: one with neat spiro-OMeTAD, and one with SWNT-spiro-OMeTAD. The charge extraction lifetime is shown in panel a. The device with the SWNT interlayer exhibits close to 1 order of magnitude faster extraction. The recombination lifetime in panel b appears to be quite similar in both devices. The faster charge extraction leads to a higher charge extraction efficiency with increasing light intensity, shown in panel c.

To further clarify how direct hole transfer from the perovskite to the nanotubes leads to an increase in efficiency, we performed small perturbation transient photocurrent decay (Figure 4).[28]

Figure 4a illustrates the charge extraction time measured at open circuit voltage plotted against various light intensities for two devices with a HTL composed either of solely spiro-OMeTAD or of the sequentially coated SWNT-spiro-OMeTAD structure. For all light intensities, it can be seen that charge extraction occurs almost 1 order of magnitude faster in the presence of the P3HT/SWNT nanohybrid interlayer.

The fact that the charge extraction lifetimes decrease with light intensity for both structures indicates that charge transport through undoped spiro-OMeTAD limits hole transport for both structures. Because we have previously demonstrated that neat spiro-OMeTAD has a strongly charge density-dependent mobility.[29] In the case of the nanotube composite structure, however, only a fraction of the photogenerated holes are transported through spiro-OMeTAD, whereas the others are extracted through the SWNTs resulting in a greatly improved

dx.doi.org/10.1021/jz5021795 | J. Phys. Chem. Lett. 2014, 5, 4207−4212

extraction rate. The observation that the recombination rate is comparable between the undoped spiro-OMeTAD layer and the nanohybrids structure (Figure 4b) indicates that the enhancement of the hole extraction throughout the HTL is the main cause for the overall improved performance. At higher light intensities in particular, the improved transport properties of the stratified HTL structure results in much higher charge collection efficiency values (defined as the ratio of extraction rate to the sum of extraction and recombination rate) (Figure 4c). This is in agreement with a linear dependence of the short-circuit current on light intensity (Supporting Information).

In summary, we have shown that P3HT-wrapped SWNTs act as highly effective p-type charge transporters in perovskite solar cells and allow us to fully replace the Li-TFSI doping of spiro-OMeTAD usually required for comparable efficiencies. Sequentially depositing nanotubes and spiro-OMeTAD is shown to be superior to blend structures, most likely because the nanotubes can form a well-connected percolation network in this configuration. This double-layer structure has the potential to become a model system for carbon nanotube based charge-collection layers, which can extract charges as well as protect vulnerable interfaces.

METHODS

SWNT Functionalization. Powdered SWNTs produced by the HiPco process were purchased from Carbon Nanotechnologies Incorporated (CNI; now Unidym) with lengths 100−1000 nm and an intermediate diameter distribution of 0.8−1.2 nm. The samples used in this work were purchased as "purified" tubes (<15 wt % iron catalyst impurities). rr-P3HT (3.0 mg; Rieke Metals Inc., weight-average molecular weight, M_w = 50 000 g mol^{-1} and regioregularity = 95%) was dissolved in 5.00 mL of chlorobenzene and sonicated in a bath sonicator for 60 min. Purified HiPco SWNTs (2.5 mg) were added as purchased to the dissolved polymer solution and treated with an ultrasonic probe for 10 min. The mixture was subsequently centrifuged for 8 min at 10 000*g* to remove nonfunctionalized SWNTs and other carbonaceous particles. The precipitate was discarded, while the supernatant was recovered. In order to remove the excess polymer according to the solvent extraction technique detailed by Schuettforth et al.,[10] 15 mL of toluene was added. The mixture was then mildly heated for 60 min to induce aggregation of the functionalized SWNTs. The aggregates were then removed by centrifugation (4 min at 16 000*g*). This time the supernatant containing excess polymer was discarded, and the precipitate was recovered and redispersed in 5 mL of toluene. This mixture was then sonicated for 15 min in the ultrasonic bath to fully redisolve nonwrapped polymers. After the sonication, the mixture was mildly heated for 15 min to induce aggregation and then centrifuged for 4 min at 16 000*g*. The supernatant was then discarded. This procedure from bath sonication to centrifugation was repeated three times to remove all excess polymer resulting in the final supernatant being fully transparent. The final pellet consists of 2.0−2.2 mg of functionalized nanotubes, which are dispersed in 16 mL chloroform. Immediately prior to spin-casting, the chloroform solution was sonicated with an ultrasonic probe for 2 min at low intensity to break up clusters and bundles.

Solar Cell Fabrication. A glass wafer with a layer of FTO was first cleaned with detergent and deionized water, then with acetone and isopropanol. Thereafter it was treated for 10 min in O_2 plasma. The electron-accepting TiO_2 compact layer was spin-coated (2000 rpm for 60 s) from a mildly acidic (after addition of 12 μM HCl) solution of titanium isopropoxide in anhydrous ethanol and sintered at 500 °C. The low-temperature meso-structured scaffold was afterward deposited by spin-coating (2500 rpm for 60s) from a colloidal dispersion of 50 nm Al_2O_3 nanoparticles in isopropanol followed by drying at 150 °C.[3] After having cooled down to room temperature, the perovskite layer was spin-cast and dried at 100 °C for 45 min. Following this step, the hole transport layer was deposited by spin-coating. For the two-layer structure of SWNT and polymer, first the SWNT layer was deposited dynamically by slow drop-by-drop spin-coating (3000 rpm for 90 s) of 200 μL. Followed immediately by the deposition of the spiro-OMeTAD [90 mg/mL in chlorobenzene] layer by spin-coating (2000 rpm for 60 s). After removing the HTL and the active layer at the bottom of the device, bottom and top electrodes were deposited by thermal evaporation of 150 nm of Ag.

Current−Voltage Measurements. For measuring the performance of the solar cells, simulated AM 1.5 sunlight was generated with a class AAB ABET solar simulator calibrated to give simulated AM 1.5 of 100.0 mW cm^{-2} equivalent irradiance, using an NREL-calibrated KG5 filtered silicon reference cell. The mismatch factor was calculated to be 1.02 between 300 to 900 nm, which is greater than the operating range of both the KG5 filtered silicon reference cell and the perovskite test cells.[3] The current−voltage curves were recorded with a sourcemeter (Keithley 2400, USA). The solar cells were masked with a metal aperture defining the active area (0.063 cm^2) of the solar cells. Additionally, by removing active material between individual cells cross-talk between neighboring cells was prevented. Measurements were done in a light-tight sample holder to minimize any edge effects and ensure that the reference cell and test cell are located during measurement in the same spot under the solar simulator.

Photoinduced Absorption Spectroscopy. PIA spectra were obtained from full device structures with varying hole transport layer architectures. These samples were excited with an argon ion laser with a wavelength of 515 nm with a maximum fluence of 50 mW/cm^2 and chopped at a frequency of 23 Hz. The optical probe is in the form of a white light halogen bulb of around 1 sun intensity. After passing through the sample, the probe beam enters a monochromator (SpectraPro-2300i, Acton Research Corporation) coupled to a diode for detection in the visible (PDA10A, Thorlabs) and in the near-IR (ID-441-C, Acton Research Corporation). Acquisition is made by a lock-in amplifier locked at the light modulation frequency (SR830, Stanford Research Systems) and a NI USB-6008 (National Instruments) acquisition card. A computer running LabView (National Instruments) controls the setup and record spectra. No further treatment is applied to the data.

ASSOCIATED CONTENT

Supporting Information

Energy scheme, role of P3HT, spiro-OMeTAD concentration, stability, stabilized power-output and short-circuit current dependence on light intensity can be found in the Supporting Information. This material is available free of charge via the Internet at http://pubs.acs.org.

AUTHOR INFORMATION

Corresponding Author

*E-mail: h.snaith1@physics.ox.ac.uk.

Author Contributions

All authors contributed to the writing of the manuscript. S.N.H. conceived and carried out the experiments with help from T.L., G.E.E., and S.D.S.; H.J.S. and R.J.N. conceived and supervised the project. All authors discussed the results and commented on the manuscript.

Notes

The authors declare no competing financial interest.

■ ACKNOWLEDGMENTS

This work was partly funded by the European Community's Seventh Framework Programme (FP7/2007−2013) under Grant Agreement No. 246124 of the SANS project and by the Engineering and Physical Sciences Research Council.

■ REFERENCES

(1) Snaith, H. J. Perovskites: The Emergence of a New Era for Low-Cost, High-Efficiency Solar Cells. *J. Phys. Chem. Lett.* **2013**, 3623−3630.

(2) Lotsch, B. V. New Light on an Old Story: Perovskites Go Solar. *Angew. Chem., Int. Ed.* **2014**, *53*, 635−637.

(3) Ball, J. M.; Lee, M. M.; Hey, A.; Snaith, H. J. Low-Temperature Processed Meso-Superstructured to Thin-Film Perovskite Solar Cells. *Energy Environ. Sci.* **2013**, *6*, 1739.

(4) Lee, M. M.; Teuscher, J.; Miyasaka, T.; Murakami, T. N.; Snaith, H. J. Efficient Hybrid Solar Cells Based on Meso-Superstructured Organometal Halide Perovskites. *Science* **2012**, *338*, 643−647.

(5) Stranks, S. D.; Eperon, G. E.; Grancini, G.; Menelaou, C.; Alcocer, M. J. P.; Leijtens, T.; Herz, L. M.; Petrozza, A.; Snaith, H. J. Electron-Hole Diffusion Lengths Exceeding 1 Micrometer in an Organometal Trihalide Perovskite Absorber. *Science* **2013**, *342*, 341−344.

(6) Dualeh, A.; Moehl, T.; Nazeeruddin, M. K.; Grätzel, M. Temperature Dependence of Transport Properties of Spiro-MeOTAD as a Hole Transport Material in Solid-State Dye-Sensitized Solar Cells. *ACS Nano* **2013**, *7*, 2292−2301.

(7) Abate, A.; Hollman, D. J.; Teuscher, J.; Pathak, S.; Avolio, R.; D'Errico, G.; Vitiello, G.; Fantacci, S.; Snaith, H. J. Protic Ionic Liquids as P-Dopant for Organic Hole Transporting Materials and Their Application in High Efficiency Hybrid Solar Cells. *J. Am. Chem. Soc.* **2013**, *135*, 13538−13548.

(8) Burschka, J.; Dualeh, A.; Kessler, F.; Baranoff, E.; Cevey-Ha, N.-L.; Yi, C.; Nazeeruddin, M. K.; Grätzel, M. Tris(2-(1H-pyrazol-1-yl)pyridine)cobalt(III) as P-Type Dopant for Organic Semiconductors and Its Application in Highly Efficient Solid-State Dye-Sensitized Solar Cells. *J. Am. Chem. Soc.* **2011**, *133*, 18042−18045.

(9) Habisreutinger, S. N.; Leijtens, T.; Eperon, G. E.; Stranks, S. D.; Nicholas, R. J.; Snaith, H. J. Carbon Nanotube/Polymer Composites as a Highly Stable Charge Collection Layer in Perovskite Solar Cells. *Nano Lett.* **2014**, *14*, 5561−5568.

(10) Schuettfort, T.; Snaith, H. J.; Nish, A.; Nicholas, R. J. Synthesis and Spectroscopic Characterization of Solution Processable Highly Ordered Polythiophene−Carbon Nanotube Nanohybrid Structures. *Nanotechnology* **2010**, *21*, 25201.

(11) Dissanayake, N. M.; Zhong, Z. Unexpected Hole Transfer Leads to High Efficiency Single-Walled Carbon Nanotube Hybrid Photovoltaic. *Nano Lett.* **2011**, *11*, 286−290.

(12) Dabera, G. D. M. R.; Jayawardena, K. D. G. I.; Prabhath, M. R. R.; Yahya, I.; Tan, Y. Y.; Nismy, N. A.; Shiozawa, H.; Sauer, M.; Ruiz-Soria, G.; Ayala, P.; et al. Hybrid Carbon Nanotube Networks as Efficient Hole Extraction Layers for Organic Photovoltaics. *ACS Nano* **2013**, *7*, 556−565.

(13) Etgar, L.; Gao, P.; Xue, Z.; Peng, Q.; Chandiran, A. K.; Liu, B.; Nazeeruddin, M. K.; Grätzel, M. Mesoscopic $CH_3NH_3PbI_3/TiO_2$ Heterojunction Solar Cells. *J. Am. Chem. Soc.* **2012**, *134*, 17396−17399.

(14) Marchioro, A.; Teuscher, J.; Friedrich, D.; Kunst, M.; van de Krol, R.; Moehl, T.; Grätzel, M.; Moser, J.-E. Unravelling the Mechanism of Photoinduced Charge Transfer Processes in Lead Iodide Perovskite Solar Cells. *Nat. Photonics* **2014**, 1−6.

(15) Dürkop, T.; Getty, S. A.; Cobas, E.; Fuhrer, M. S. Extraordinary Mobility in Semiconducting Carbon Nanotubes. *Nano Lett.* **2004**, *4*, 35−39.

(16) Martel, R.; Derycke, V.; Lavoie, C.; Appenzeller, J.; Chan, K.; Tersoff, J.; Avouris, P. Ambipolar Electrical Transport in Semiconducting Single-Wall Carbon Nanotubes. *Phys. Rev. Lett.* **2001**, *87*, 256805.

(17) Hong, S.; Myung, S. Nanotube Electronics: A Flexible Approach to Mobility. *Nat. Nanotechnol.* **2007**, *2*, 207−208.

(18) Spitalsky, Z.; Tasis, D.; Papagelis, K.; Galiotis, C. Carbon Nanotube−Polymer Composites: Chemistry, Processing, Mechanical and Electrical Properties. *Prog. Polym. Sci.* **2010**, *35*, 357−401.

(19) Bauhofer, W.; Kovacs, J. Z. A Review and Analysis of Electrical Percolation in Carbon Nanotube Polymer Composites. *Compos. Sci. Technol.* **2009**, *69*, 1486−1498.

(20) Wang, J. T.-W.; Ball, J. M.; Barea, E. M.; Abate, A.; Alexander-Webber, J. A.; Huang, J.; Saliba, M.; Mora-Sero, I.; Bisquert, J.; Snaith, H. J.; et al. Low-Temperature Processed Electron Collection Layers of Graphene/TiO_2 Nanocomposites in Thin Film Perovskite Solar Cells. *Nano Lett.* **2014**, *14*, 724−730.

(21) Wojciechowski, K.; Saliba, M.; Leijtens, T.; Abate, A.; Snaith, H. J. Sub-150 °C Processed Meso-Superstructured Perovskite Solar Cells with Enhanced Efficiency. *Energy Environ. Sci.* **2014**, *7*, 1142−1147.

(22) Snaith, H. J.; Abate, A.; Ball, J. M.; Eperon, G. E.; Leijtens, T.; Noel, N. K.; Stranks, S. D.; Wang, J. T.; Wojciechowski, K.; Zhang, W. Anomalous Hysteresis in Perovskite Solar Cells. *J. Phys. Chem. Lett.* **2014**, *5*, 1511−1515.

(23) Unger, E. L.; Hoke, E. T.; Bailie, C. D.; Nguyen, W. H.; Bowring, A. R.; Heumuller, T.; Christoforo, M. G.; McGehee, M. D. Hysteresis and Transient Behavior in Current−Voltage Measurements of Hybrid-Perovskite Absorber Solar Cells. *Energy Environ. Sci.* **2014**, *7*, 3690−3698.

(24) Kim, H.-S.; Lee, C.-R.; Im, J.-H.; Lee, K.-B.; Moehl, T.; Marchioro, A.; Moon, S.-J.; Humphry-Baker, R.; Yum, J.-H.; Moser, J. E.; et al. Lead Iodide Perovskite Sensitized All-Solid-State Submicron Thin Film Mesoscopic Solar Cell with Efficiency Exceeding 9%. *Sci. Rep.* **2012**, *2*, 591.

(25) Bi, D.; Yang, L.; Boschloo, G.; Hagfeldt, A.; Johansson, E. M. J. Effect of Different Hole Transport Materials on Recombination in $CH_3NH_3PbI_3$ Perovskite-Sensitized Mesoscopic Solar Cells. *J. Phys. Chem. Lett.* **2013**, *4*, 1532−1536.

(26) Weisman, R. B.; Bachilo, S. M. Dependence of Optical Transition Energies on Structure for Single-Walled Carbon Nanotubes in Aqueous Suspension: An Empirical Kataura Plot. *Nano Lett.* **2003**, *3*, 1235−1238.

(27) Kimoto, Y.; Okano, M.; Kanemitsu, Y. Observation of Excited-State Excitons and Band-Gap Renormalization in Hole-Doped Carbon Nanotubes Using Photoluminescence Excitation Spectroscopy. *Phys. Rev. B* **2013**, *87*, 195416.

(28) O'Regan, B. C.; Lenzmann, F. Charge Transport and Recombination in a Nanoscale Interpenetrating Network of N-Type and P-Type Semiconductors: Transient Photocurrent and Photovoltage Studies of TiO_2/Dye/CuSCN Photovoltaic Cells. *J. Phys. Chem. B* **2004**, *108*, 4342−4350.

(29) Leijtens, T.; Lim, J.; Teuscher, J.; Park, T.; Snaith, H. J. Charge Density Dependent Mobility of Organic Hole-Transporters and Mesoporous TiO_2 Determined by Transient Mobility Spectroscopy: Implications to Dye-Sensitized and Organic Solar Cells. *Adv. Mater.* **2013**, *25*, 3227−3233.